3852 *Macromolecules* **2009**, *42*, 3852–3855
DOI: 10.1021/ma900622s

Macromolecules
COMMUNICATION TO THE EDITOR

Direct Observation of Damage Zone around Crack Tips in Double-Network Gels

Qiu Ming Yu, Yoshimi Tanaka, Hidemitsu Furukawa, Takayuki Kurokawa, and Jian Ping Gong*

Department of Biological Sciences, Graduate School of Science, Hokkaido University, N10W8, Sapporo 060-0810, Japan

Received March 23, 2009
Revised Manuscript Received May 21, 2009

Most hydrogels derived from natural or synthetic sources have low mechanical strength.[1] In 2003, we succeeded in developing novel hydrogels with extremely high mechanical strength by introducing a double-network structure (DN), consisting of a densely cross-linked polyelectrolyte gel and a loosely cross-linked neutral network.[2] Even though DN gels contain about 90% water, the fracture energy G ranges from 10^2 to 10^3 J/m^2, which is 100−1000 times larger than that of normal polyacrylamide (PAAm) gels (10 J/m^2) or poly(2-acrylamido-2-methylpropanesulfonic acid) (PAMPS) gels (10^{-1} J/m^2) whose polymer concentrations are similar to those of DN gels.[3−5] Because of the anomalously high mechanical strength and high water content of DN gels, they are expected to have various applications, especially in the field of regenerative medicine (for fabricating artificial tissues and cartilage, etc.).[6−8]

The fundamental toughening mechanism of DN gels is of great interest to researchers. Several experimental and theoretical studies have been performed to explain this mechanism.[4,5,9−14] Necking deformation[9] that was observed through tensile tests and rate-independent hysteresis[13] observed through cyclic loading tests have indicated that DN gels can accumulate internal damage before the suffering macroscopic fracture; after damage accumulation, the DN gels become much softer. We assume that on the microscopic level yielding is caused by the partial breakage and fragmentation of the brittle first network and interconnection among the fragments by the polymer chains of second network.[9] Brown[10] and Tanaka[12] have proposed similar models that can qualitatively explain the anomalously high fracture energy, assuming that the DN gel is locally damaged around the crack tip and that the energy dissipated for damage accumulation enhances the effective fracture energy. According to their models, the size of the damage zone could reach the order of several hundred μm, while the fracture energy could reach the order of several hundred J/m^2.[9] Using AFM measurements,[15] we successfully detected the existence of softened regions just below the fracture surfaces, which supports the assumption of localized damage accumulation. However, direct observation of the damage zone, especially, the estimation of its thickness from the crack surface, should be performed in order to confirm the assumptions of the models. In this paper, we report the direct observation of the crack tips of DN gels for the first time to ascertain the existence of the damage zone and to determine its thickness. We also compare experimental results with the results from the models.

DN hydrogels were synthesized from 2-acrylamido-2-methylpropanesulfonic acid (AMPS; Tokyo Kasei Co., Ltd.) and acrylamide (AAm; Junsei Chemical Co. Ltd.) by using the two-step free-radical polymerization method.[2] Briefly, 4 mol % (the mole percent was determined with respect to the AMPS monomer) of N,N′-methylenebis(acrylamide) (MBAA; Tokyo Kasei Co., Ltd.), which is a cross-linking agent, and 0.1 mol % of 2-oxoglutaric acid (Wako Pure Chemical Industries, Ltd.), which is a radical initiator for the gelation reactions, were added to a 1 mol/L AMPS aqueous solution. The pregel solution was poured into molds consisting of two glass plates separated by a silicone spacer. A plate of PAMPS gel was synthesized by UV irradiation to the solution in an argon atmosphere. Subsequently, the obtained PAMPS gel was immersed in a large amount of aqueous solution of the AAm monomer (2 mol/L) and 2-oxoglutaric acid (0.01 mol %). After the equilibrium swelling of the first network PAMPS gel occurred (time taken >60 h), acrylamide was polymerized in situ. The prepared DN gels were washed thoroughly in excess water to remove residual chemicals.

Tearing and tensile tests were performed using a commercial test machine (Tensilon RTC-1150A, Orientec Co.). In order to prepare specimens for the tearing experiment, the gels were cut using a gel cutting machine (Dumb Bell Co., Ltd.) into the shape specified by JISK 6252 as 1/2 sizes (50 mm×7.5 mm× 5−5.5 mm, with an initial notch of 20 mm). The two arms of the test sample were clamped and one arm was pulled upward at a velocity V, while the other arm was maintained stationary. The tearing force F was recorded. G is calculated by dividing the average of F during tearing by the width of the gel samples.[3−5,16] The tearing velocity V (crack tip velocity is $V/2$) was changed from 1×10^{-1} to 5×10^2 mm/min. For the tensile tests, samples were cut using the gel cutting machine into dumbbell shapes standardized as JIS K 6251-6 sizes (dowel width 7 mm, dowel thickness 2−3 mm, and dowel length 50 mm; bell width 4 mm, bell thickness 2−3 mm, and bell length 20 mm). The strain rate was changed from 0.5 to 25 min^{-1}.

For microscopic observation around the crack tips, the tearing was stopped at the middle of the specimen, and the specimen was immersed in water for more than 2 days. Then, the region around the crack tip was observed using a conventional optical microscope (CKX-21PHP, Olympus Co., Ltd.) and a color 3D violet laser scanning microscope (VK-9700, KEYENCE Co., Ltd.).

Figure 1a is a photographic image of a crack tip ($V=$ 0.2 mm/min) observed using the conventional optical microscope with transmission mode. Figure 1b shows a high−low image of the same crack tip captured using a color 3D violet laser scanning microscope with reflection mode. A special zone that looks different from the other regions can be observed around the crack in the images. This indicates the existence of a damage zone. Figure 1c is a schematic representation of the formation of the damage zone.[12] The advantage of using the violet laser scanning microscope is that the damage zone and its boundary appear very clearly. This feature allows the estimation of the thickness of the damage zone h. In Figure 1b, we determined the thickness of the damage zone h as 220 μm. The order of h is consistent with the predictions of previously reported models that the thickness of the damage zone could reach the order of several hundred micrometers.[12]

Two aspects of the microscopic observation should be noted here. (1) The thickness of the damage zone h was determined after immersing the cracked specimens in water. Without performing this treatment, the damage zone could not be easily observed. When a DN gel that underwent necking deformation throughout

*Corresponding author: Fax 81-11-706-2635; e-mail gong@sci.hokudai.ac.jp.

 Published on Web 05/29/2009

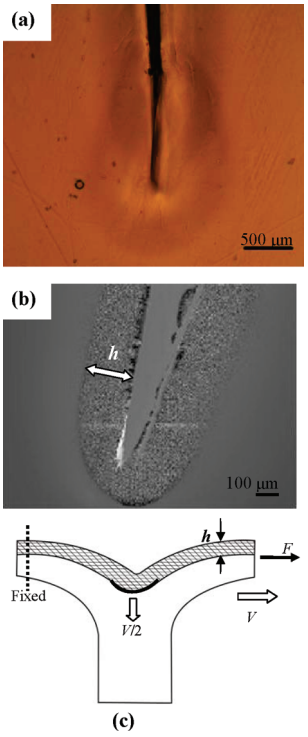

Figure 1. Images of the crack tip observed after tearing: (a) photographic image captured using a conventional optical microscope; (b) high−low image captured using a color 3D violet laser scanning microscope; (c) illustration of the damage zone (grid) and the undamage zone (blank). V is tear velocity, F the tear force, and h the thickness of damage zone.

the whole specimen was immersed in water, it swelled up. The ratio of the linear dimensions after and before swelling was less than two in the direction of tensile deformation. For the damage zone around the crack tip, the extent of swelling should be smaller than in the case of a necked gel sample because of the constraint provided by the undamage region. Therefore, we assumed that the measured value of h was not very different from the real thickness of the damage zone before swelling. (2) The violet laser scanning microscope system that used to determine h was originally designed to obtain the precise height profile of a complex surface by using a short-wavelength violet laser and an automatic focusing system. The principle to observe the damage zone using this system is discussed in the Appendix.

Figure 2a shows the dependence of fracture energy G and the thickness of the damage zone h on the tearing velocity V. Both G and h increased with V. As V changed from 1×10^{-1} to 5×10^{2} mm/min (almost 4 orders of magnitude), G just increased by several times. This is consistent with the point that G is not very sensitive to changes in V.[3] Further, for the whole velocity range investigated, the values of h ranged from 150 to 700 μm. These are consistent with the predictions based on the previous theories[10,12] that the thickness of the damage zone h could reach the order of several hundred μm when the fracture energy G reaches the order of several hundred J/m^2. Moreover, the dependence of G and that of h on V agree with each other. In Figure 2b, the relationship between G and h is shown using the same data. It can be seen that G is proportional to h, as follows:

$$G = Ah \tag{1}$$

where A is a constant representing the slope in Figure 2b. Through linear fitting, A is found to be 0.91×10^{6} N/m^2.

We compare these experimental findings with those obtained on the basis of the previous theory below.

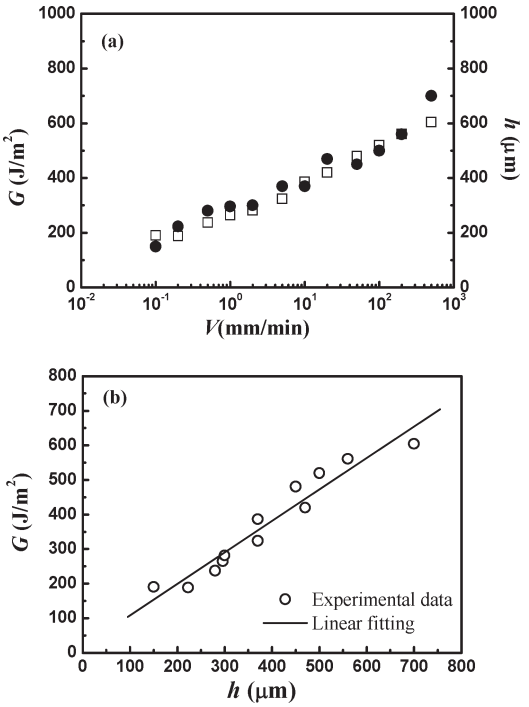

Figure 2. (a) Dependence of fracture energy (G, blank square) and the thickness of the damage zone (h, solid circle) on the tearing velocity. (b) Relationship between fracture energy (G) and the thickness of the damage zone (h).

In our previous theory, we made two basic assumptions: (i) the highly stretched region ahead of the crack tip becomes a softer damaged material at σ_c, and (ii) the local yielding behavior is almost identical to the macroscopic necking in tensile tests. In the prediction, the size of the damage zone h is given by

$$h \cong \frac{G_0}{W} \tag{2}$$

where G_0 is the intrinsic fracture energy (J/m^2) of the damaged gel and W is the characteristic elastic energy density (J/m^3) around the crack tip. The effective fracture energy G consists of the intrinsic fracture energy of the damaged gel G_0 and a dissipation term representing the formation of the damage zone; the dissipation term is given by $k\sigma_c\varepsilon_c h$, where k is the geometrical factor and ε_c is the strain of the damage zone before hardening at a yielding stress σ_c. Since $k\sigma_c\varepsilon_c h \gg G_0$

$$G \approx k\sigma_c\varepsilon_c h \tag{3}$$

It appears that eq 3 is consistent with eq 1 and can explain the proportionality between G and h. Furthermore, it can be inferred that the slope A in Figure 2b is equivalent to $k\sigma_c\varepsilon_c$.

In order to estimate the values of σ_c and ε_c on the basis of assumption ii, tensile tests at different strain rates were carried out on the dumbbell specimens. In Figure 3, it can be seen that for all strain rates the DN gels yielded to form a necked zone and σ_c was insensitive to strain rate. The plateau in Figure 3 indicates the coexistence of necked and unnecked regions. The strain ε_c can be estimated as the global strain at the right end of the plateau region before hardening occurs. The necked zone covered the whole specimen at a strain rate of 5 min^{-1}, and ε_c was ~6.4, as shown in Figure 3. Unfortunately, for other strain rates, the specimens failed while in the state corresponding to the plateau region (coexisting necked and unnecked states), and we were unable to estimate ε_c.

If we ignore the geometrical effect ($k \approx 1$) and use the values of σ_c (≈0.82 MPa) and ε_c (≈6.4) obtained from the macroscopic

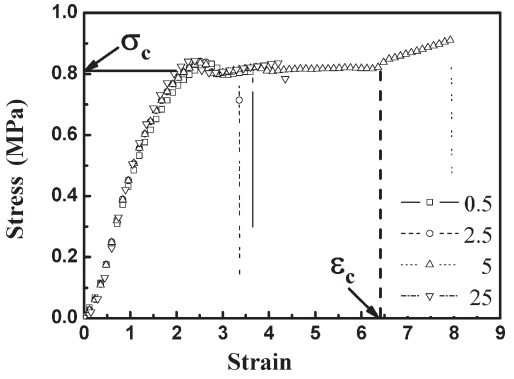

Figure 3. Loading curves of DN gels during the tensile tests at different strain rates (0.5, 2.5, 5, and 2 min^{-1}). ε_c is the strain at the end of the necking region with a constant stress σ_c.

necking tests, we can estimate that the value of $k\sigma_c\varepsilon_c$ in eq 3 is $\approx 5.25\times10^6$ N/m^2. This is, however, 6 times larger than A in eq 1, which was found to be 0.91×10^6 N/m^2 through linear fitting.

Possible reasons for the discrepancy between the results obtained from the model and experimental observations are discussed below.

(1) Damage accumulation before yielding. In the model, the process before yielding point is assumed to be ideally elastic. However, in reality, damage accumulation of the first polyelectrolyte (PAMPS) network occurs even under very small strain,[13] owing to the heterogeneity of the PAMPS network.[17] That is, even when the stress is much lower than σ_c, microscopic damage in the PAMPS network occurs. Actually, we observed uniaxially tested damaged samples at different extensions. Even for the samples extended to 2 times ($\varepsilon = 1$, before yielding point), a similar dark image with that of the tearing test as shown in Figure 1b was observed. It indicates that the damage is visible even for small strains before yielding. Therefore, the damage zone we observed for the tearing test sample includes the part occurred in the small strain before yielding. That is, the thickness of the damage zone h determined by using the color 3D violet laser scanning microscope includes this diffused damage zone. Thus, it is larger than the result obtained from the model. This gives a smaller value of G/h in the observation.

(2) Surface effect. It is well-known that during the fracture of metals the yield zone at the free surface develops more extensively than the bulk underneath.[18] Analogous behavior was also observed in several glassy polymers such as polycarbonate.[19] A thin line of material called shear lip forms on the fracture surface where the polymer yields. In DN gel specimens with necking undergoing tearing, a larger yielding zone might also be formed at the free surface. This also gives a smaller value of G/h in the observation. A factor of 2 is possible but not more.

(3) Swelling effect. We assumed that the thickness h that was observed using swollen specimens was not very different from but slightly larger than the real value before swelling. This might have also resulted in the overestimation of h and give a smaller value of G/h in observation.

Further, it should also be noted that the difference in fracture geometry (tearing tests to obtain G and necking experiments to obtain σ_c and ε_c) might have led to the condition $k \neq 1$, and this should also be taken into consideration.

In summary, the localized damage zone around the crack tip of the DN gel was successfully observed for the first time. Further, it was found that there is a proportional relationship between the thickness of the damage zone h and the fracture energy G. The quantification of the damage zone is important for further understanding the mechanism underlying the abnormal strength of DN gels.

Acknowledgment. This study was supported by a Grant-in-Aid for Specially Promoted Research (No. 18002002) from the Ministry of Education, Science, Sports and Culture of Japan. The authors thank Prof. Y. Uraki at Hokkaido University for providing the color 3D violet laser scanning microscope.

Appendix. The 3D laser scanning microscope system scans the field of the microscope using a short waveform laser beam and an $X-Y$ scan optical system. The microscope scans with the laser beam in X and Y directions in the field of view. The light receiving element detects reflecting light from each pixel of $X-Y$ position in the field of view (1024 × 768 pixels). Then the objective lens is driven in the Z-axis, and the laser scans again. Repeat scanning in the whole Z measurement range obtains reflecting light intensity based on the Z position (shown in Figure S1a). When focusing on the surface position, the maximum reflecting light intensity is detected. By determining the height information (Z) at the maximum reflection intensity (Z_{max}) for each pixel, surface profile is obtained. Consequently, the laser scanning microscope system obtains data for omnifocal light intensity ultradepth images (Figure S2a) and high−low images (Figure S2c and Figure 1b) at the Z_{max}-position. The maximum reflection intensity (I_{max}) profile and the corresponding height position (Z_{max}) profile on the line of light intensity ultradepth image (Figure S2a) and the high−low image (Figure S2c) are also shown in Figures S2b and S2d, respectively. It can be seen that the damage zone was dark, indicating a very low intensity of the reflective light, and the roughness in this zone could not be measured, as indicated by the strong fluctuation in the height profile as shown in Figure S1b. However, the actual surface of the damage zone, as revealed by the conventional optical microscope (Figure 1a), was as smooth as the undamage region. Therefore, the dark image in Figure 1b is due to the enhanced static fluctuation or inhomogeneity of the refractive index in the damage zone which leads to the diffusive reflection of the laser light. This also explains why the damage zone cannot be observed when we observe the sample in the as-fractured state without swollen in water. As a conclusion, the damage zone observed in Figure 1b is due to the scattering of light by the inhomogeneous structure beneath the surface of the damage zone.

Supporting Information Available: Measurement principle of 3D laser microscope system for damage zone. This material is available free of charge via the Internet at http://pubs.acs.org.

References and Notes

(1) Tanaka, Y.; Fukao, K.; Miyamoto, Y. *Eur. J. Phys. E* **2000**, *3*, 395.
(2) Gong, J. P.; Katsuyama, Y.; Kurokawa, T.; Osada, Y. *Adv. Mater.* **2003**, *15*, 1155.
(3) Tanaka, Y.; Kuwabara, R.; Na, Y. H.; Kurokawa, T.; Gong, J. P.; Osada, Y. *J. Phys. Chem. B* **2005**, *109*, 11559.
(4) Tsukeshiba, H.; Huang, M.; Na, Y.-H.; Kurokawa, T.; Kuwabara, R.; Tanaka, Y.; Furukawa, H.; Osada, Y.; Gong, J. P. *J. Phys. Chem. B* **2005**, *109*, 16304.
(5) Huang, M.; Furukawa, H.; Tanaka, Y.; Nakajima, T.; Osada, Y.; Gong, J. P. *Macromolecules* **2007**, *40*, 6658.
(6) Kurokawa, T.; Tominaga, T.; Katsuyama, Y.; Kuwabara, R.; Furukawa, H.; Osada, Y.; Gong, J. P. *Langmiur* **2005**, *21*, 8643.
(7) Tanabe, Y.; Yasuda, K.; Azuma, C.; Taniguro, H.; Onodera, S.; Suzuki, A.; Chen, Y. M.; Gong, J. P.; Osada, Y. *J. Mater. Sci.: Mater. Med.* **2008**, *19*, 1379.

(8) Yasuda, K.; Kitamura, N.; Gong, J. P.; Arakaki, K.; Kwon, H. J.; Onodera, S.; Chen, Y. M.; Kurokawa, T.; Kanaya, F.; Ohmiya, Y.; Osada, Y. *Macromol. Biosci.*, published online.
(9) Na, Y. H.; Tanaka, Y.; Kawauchi, Y.; Furukawa, H.; Sumiyoshi, T.; Gong, J. P.; Osada, Y. *Macromolecules* **2006**, *39*, 4641.
(10) Brown, H. R. *Macromolecules* **2007**, *40*, 3815.
(11) Shull, K. R. *J. Polym. Sci., Part B: Polym. Phys.* **2006**, *44*, 3436.
(12) Tanaka, Y. *Europhys. Lett.* **2007**, *78*, 56005.
(13) Webber, R. E.; Creton, C.; Brown, H. R.; Gong, J. P. *Macromolecules* **2007**, *40*, 2919.
(14) Miquelard-Garnier, G.; Demoures, S.; Creton, C.; Hourdet, D. *Macromolecules* **2006**, *39*, 8128.
(15) Tanaka, Y.; Kawauchi, Y.; Kurokawa, T.; Furukawa, H.; Okajima, T.; Gong, J. P. *Macromol. Rapid Commun.* **2008**, *29*, 1514.
(16) Furukawa, H.; Kuwabara, R.; Tanaka, Y.; Kurokawa, T.; Na, Y. H.; Osada, Y.; Gong, J. P. *Macromolecules* **2008**, *41*, 7173.
(17) Tominaga, T.; Tirumala, V. R.; Lee, S.; Lin, E. K.; Gong, J. P.; Wu, W. l. *J. Phys. Chem. B* **2008**, *112*, 3903.
(18) Anderson, T. L. *Fracture Mechanics: Fundamentals and Application*; Taylor & Francis: London, 2005; p 273.
(19) Ward, I. M.; Sweeney, J. *An Introduction to the Mechanical Properties of Solid Polymers*; John Wiley & Sons: New York, 2004; p 285.